J. Fluid Mech. (2001), *vol.* 447, *pp.* 173–177. © 2001 Cambridge University Press
DOI: 10.1017/S0022112001005833 Printed in the United Kingdom

A note on surface waves generated by shear-flow instability

By JOHN MILES

Cecil H. and Ida M. Green Institute of Geophysics and Planetary Physics, University of California, San Diego, La Jolla, CA 92093-0225, USA

(Received 13 February 2001 and in revised form 23 May 2001)

Morland, Saffman & Yuen's (1991) study of the stability of a semi-infinite, concave shear flow bounded above by a capillary–gravity wave, for which they obtained numerical solutions of Rayleigh's equation, is revisited. A variational formulation is used to construct an analytical description of the unstable modes for the exponential velocity profile $U = U_0 \exp(y/d)$, $-\infty < y \leqslant 0$. The assumption of slow waves ($|c| \ll U_0$) yields an approximation that agrees with the numerical results of Morland *et al.* The assumption of short waves ($kd \gg 1$) yields Shrira's (1993) asymptotic approximation.

1. Introduction

Morland, Saffman & Yuen (1991, hereinafter referred to as MSY), consider the stability of a semi-infinite, smooth, monotonic ($U' > 0$) concave ($U'' > 0$) shear flow $U(y)$ bounded above by a straight-crested capillary–gravity wave. They were motivated by the conjecture 'that when a sufficiently strong wind picks up over [an initially] calm body of water … vorticity diffuses into the fluid from the surface and … waves spontaneously appear due to the instability of the [wind-induced] fluid flow …' . There did not appear to be any observational support for this conjecture at that time, but Melville, Shear & Veron (1998) have since reported experiments in which 'the surface current becomes unstable to surface wave modes' following the initiation of wind in a wave tank. Moreover, the problem merits consideration in the general context of hydrodynamic stability and complements the earlier work of Burns (1953) and Yih (1972) for convex ($U'' < 0$) shear flows.

The complex amplitude $\phi(y)$ of the perturbation stream function

$$\psi(x, y, t) = \mathrm{Re}\{\phi(y)\mathrm{e}^{\mathrm{i}k(x-ct)}\}, \tag{1}$$

where k is a positive wavenumber and $c \equiv c_r + \mathrm{i}c_i$ is a complex wave speed, is governed by Rayleigh's equation

$$\phi'' - \left(k^2 + \frac{U''}{U-c}\right)\phi = 0 \quad ('\equiv \mathrm{d}/\mathrm{d}y, \quad -\infty < y < 0), \tag{2}$$

subject to the boundary conditions (T is the kinematic surface tension)

$$(U-c)^2\phi' - [U'(U-c) + g + Tk^2]\phi = 0 \quad (y = 0) \tag{3}$$

and

$$\phi \to 0 \quad (ky \downarrow -\infty). \tag{4}$$

MSY obtain numerical solutions of (2)–(4) for three smooth velocity profiles, of which the simplest is

$$U(y) = U_0 \mathrm{e}^{y/d}, \tag{5}$$

where U_0 is the surface velocity and d is a characteristic depth ($U_0 = u_d$ and $d = \Delta/2$ in MSY). Their results are qualitatively insensitive to the choice among these profiles, and each comprises a closed loop of relatively slow ($c_r/U_0 \ll 1$), unstable modes that emerges from $c = 0$ into Howard's semicircle based on $0 < c < U_0$. The instability is induced by a phase shift across the critical layer ($y = y_c$, where $U = c$). The presence of this critical layer contrasts with its absence from Burns' and Yih's smooth, convex profiles and MSY's piecewise-linear profile (for which the instability differs qualitatively from that for a smooth profile). None of these profiles possess inflection points, which introduce additional features (cf. Engevik 2000).

2. Variational approximation ($|c| \ll U_0$)

Multiplying (2) by ϕ, integrating by parts from $y = -\infty$ to $y = 0$ along a path indented under $y = y_c$ (cf. Miles 1957), and invoking (3) and (4), we obtain

$$\left[\frac{U'(U-c) + g + Tk^2}{(U-c)^2}\right]_0 \phi_0^2 - \int_{-\infty}^{0} \left[\phi'^2 + \left(k^2 + \frac{U''}{U-c}\right)\phi^2\right] \mathrm{d}y = 0 \tag{6}$$

(the subscript 0 implies $y = 0$). The quadratic form (6) is stationary with respect to variations of ϕ about the solution of (2)–(4) and provides the basis for variational approximations to $c = c(k)$.

Guided by MSY's results, we adopt the exponential profile (5) and assume that $|c/U_0| \ll 1$.† A suitable trial function then is provided by

$$\phi = \phi_0 \mathrm{e}^{\beta y/d}, \quad \beta \equiv (k^2 d^2 + 1)^{1/2}, \tag{7a,b}$$

which satisfies (2) and (4) for $c = 0$. Substituting (5) and (7) into (6) and rendering the result dimensionless, we obtain the dispersion equation

$$1 - \mathcal{c} + G[1 + C(\beta^2 - 1)] - (1 - \mathcal{c})^2[\beta + I(\beta, \mathcal{c})] \equiv D(\beta, \mathcal{c}) = 0, \tag{8}$$

where

$$\mathcal{c} = c/U_0, \quad G = gd/U_0^2, \quad C = T/gd^2 \equiv (l/d)^2, \tag{9a–c}$$

G is an inverse Froude number, C is an inverse Bond number, l is the capillary length, D is a dispersion function,

$$I(\beta, \mathcal{c}) \equiv \mathcal{c} \int_0^1 \frac{z^{2\beta-1}\,\mathrm{d}z}{z - \mathcal{c}} = -(2\beta)^{-1} F(1, 2\beta; 2\beta + 1; 1/\mathcal{c}) \tag{10a}$$

$$= (2\beta - 1)^{-1} \mathcal{c} F(1, 1 - 2\beta; 2 - 2\beta; \mathcal{c}) + \pi \mathcal{c}^{2\beta}(\mathrm{i} - \cot 2\pi\beta), \tag{10b}$$

$z = \exp(y/d)$, F is a hypergeometric function (Abramowitz & Stegun 1965, §§ 15.3.1, 7), and $\mathrm{i}\pi\mathcal{c}^{2\beta}$ is derived from the indentation under $z = \mathcal{c}$. Note that (10b) is indeterminate, but I is elementary, if $2\beta - 1$ is a positive integer.

The error in the trial function (7) is $O(\mathcal{c})$, whence an error factor of $1 + O(\mathcal{c}^2)$ is implicit in the variational approximation (8). Accordingly (although the full variational approximation (8) is worth retaining if $\mathcal{c}$ is not small), we approximate (8)

† The solution of (2)–(5) for unrestricted c/U_0 may be expressed in terms of hypergeometric functions (cf. Hughes & Reid 1965).

by

$$D(\beta, c) = D_0(\beta) + D_1(\beta)c - \mathrm{i}\pi c^{2\beta} = 0, \tag{11}$$

where

$$D_0(\beta) = \frac{(\beta - \beta_+)(\beta - \beta_-)}{\beta_+ + \beta_-}, \quad D_1(\beta) = \frac{4\beta(\beta - 1)}{2\beta - 1}, \tag{12a, b}$$

and

$$\beta_\pm = (2CG)^{-1}\{1 \pm [(1 - 2CG)^2 - 4CG^2]^{1/2}\}. \tag{12c}$$

The approximation (11) yields the complex eigenvalue

$$c = c_r + \mathrm{i}c_i, \quad c_r = \frac{(\beta - \beta_-)(\beta_+ - \beta)}{(\beta_+ + \beta_-)D_1(\beta)}, \quad c_i = \frac{\pi c_r^{2\beta}}{D_1(\beta)}, \tag{13a–c}$$

if and only if $\beta_+ > \beta_- > 1$. This requires $G < [2(C + \sqrt{C})]^{-1}$ or, equivalently,

$$U_0 > c_m[1 + (l/d)]^{1/2} \equiv U_*, \tag{14}$$

where $c_m = (2gl)^{1/2}$ is the minimum wave speed for still water. (This sharpens the condition $U_0 > c_m$ given by Caponi *et al.* 1991.) The locus of complex c (MSY's 'tongue') then is traversed from $c = 0$ as β increases from β_- along the upper branch and returns to $c = 0$ along the lower branch as β increases to β_+. This locus shrinks to $c = 0$ for $U_0 = U_*$, and $c_i = 0$ for $U_0 < U_*$. The maximum value of c_r (at the junction of the upper and lower branches) given by (13*b*) increases from 0 to $\frac{1}{2}$ as U_0/U_* increases from 1 to ∞.

3. Comparison with MSY

Consider, for example, $U_0/c_m = 2$ and $d/l = \pi/2$, for which (9*b, c*) and (12*c*) yield $C = 4/\pi^2$, $G = \pi/16$, $\beta_+ = 11.33$ and $\beta_- = 1.24$. These $\beta_\pm$ yield $\lambda/\Delta = 0.28/4.28$ for the intersections of the dotted (exponential-profile) and solid lines in MSY's figure 2(*b*) and agree with their results within the resolution of the plot. The corresponding maxima are $c_i = 5.3 \times 10^{-3}$ at $\beta = 1.5$ and $c_r = 0.243$ at $\beta = 3.1$, which compares with $c_r = 0.23$ from MSY's figure 3(*b*) (for their error-function profile). The present c_i are too small ($< 5 \times 10^{-3}$ along the upper branch and $< 10^{-4}$ along the lower branch) to resolve the locus of instability on the scale of Howard's semicircle, but we remark that this locus differs substantially from MSY's figure 1, which, however, was intended 'only ... as a qualitative sketch' (Morland, private communication).

The maximum $\mu = 0.0064$ of the dimensionless growth rate (see figure 1)

$$\mu \equiv (d/U_0)kc_i = (\beta^2 - 1)^{1/2}c_i \quad (\beta_- < \beta < \beta_+) \tag{15}$$

compares with 0.010 from MSY's figure 3(*a*) (error-function profile). The limited resolution of their plot and the difference in velocity profiles provide a plausible explanation of the discrepancy in this comparison.

The smallness of c_i suggests that the predicted instability might be annulled by viscous dissipation. The damping coefficient for waves on a clean surface is $kc_i = -2\nu k^2$ (Lamb 1932, § 348), which yields the damping ratio

$$\frac{2\nu k^2}{kc_m} = \frac{2\nu}{l(2gl)^{1/2}} = 3.0 \times 10^{-3} \tag{16}$$

for the minimum wave speed ($kl = 1$). This compares with $c_i/c_r \simeq 4 \times 10^{-2}$ in the

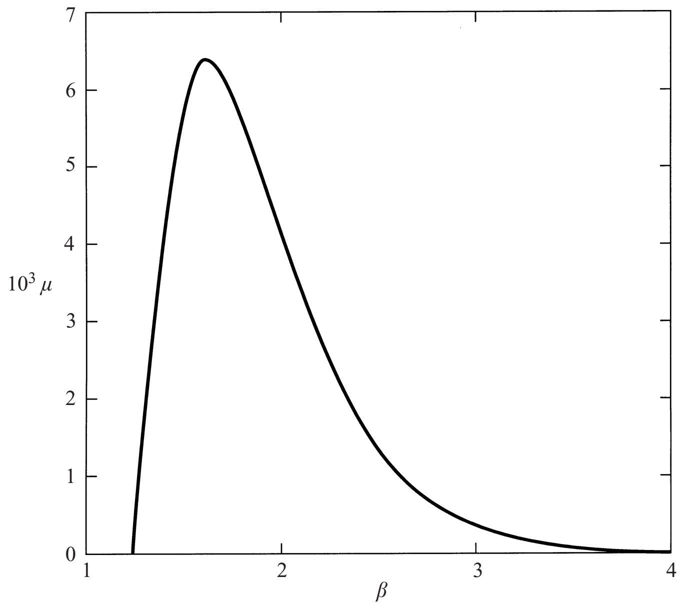

FIGURE 1. The dimensionless growth rate (15) for $U_0/c_m = 2$ and $d/l = \pi/2$ ($C = 4/\pi^2$, $G = \pi/16$, $\beta_- = 1.24$ and $\beta_+ = 11.33$). Although c_i, and therefore μ, is positive for $\beta_- < \beta < \beta_+$, it is $< 10^{-4}$ for $3.6 < \beta < \beta_+$.

neighbourhood of the maximum growth rate, but it is much larger than the damping ratio over the lower branch of the locus of instability.

4. The limit $kd \uparrow \infty$

Shrira (1993) develops the solution of (2)–(5) as an expansion in

$$\varepsilon = (k^2 c_0)^{-1}, \quad \text{where} \quad k \equiv kd \quad \text{and} \quad c_0^2 \equiv G(k^{-1} + Ck), \tag{17a–c}$$

but he gives explicit results only for his first approximation.

An alternative derivation of this first approximation follows from the adoption of the asymptotic approximation (which corresponds to potential flow)

$$\phi \sim \phi_0 \mathrm{e}^{ky} \quad (k \uparrow \infty) \tag{18}$$

as a trial function in (6). Proceeding as in §2 and invoking (9a–c), (17b,c) and $z = \exp(y/d)$, we obtain

$$\frac{1 - c + k c_0^2}{(1-c)^2} = k + \int_0^1 \frac{z^{2k}\,\mathrm{d}z}{z - c} \sim k + \pi \mathrm{i} c^{2k} + O(k^{-1}), \tag{19}$$

which yields (cf. (13b,c) and (15))

$$c_r = 1 - c_0 - \tfrac{1}{2}k^{-1} + O(k^{-2}), \quad c_i = \frac{\pi c_0 c_r^{2k}}{2k}[1 + O(k^{-2})], \quad \mu = k c_i, \tag{20a–c}$$

in agreement with Shrira's results, in particular his (5.1). The threshold of instability, maximum growth rate, and short-wave cutoff calculated from (20) are $k_- = 1.05$, $\mu_{max} = 3.7 \times 10^{-3}$ at $k = 1.6$ and $k_+ = 11.26$, which compare with $k_- = 0.73$, $\mu_{max} = 6.4 \times 10^{-3}$ at $k = 0.76$ and $k_+ = 11.29$ from (13) and (15).

This work was supported in part by the Division of Ocean Sciences of the National Science Foundation Grant OCE98-03204, and by the Office of Naval Research Grant N00014-92-J-1171.

REFERENCES

Abramowitz, M. & Stegun, I. A. 1965 *Handbook of Mathematical Functions*. U.S. National Bureau of Standards.

Burns, J. C. 1953 Long waves in running water. *Proc. Camb. Phil. Soc.* **49**, 695–706.

Caponi, E. A., Yuen, H. C., Milinazzo, F. A. & Saffman, P. G. 1991 Water wave instability induced by a drift layer. *J. Fluid Mech.* **222**, 297–313.

Engevik, L. 2000 A note on the instabilities of a horizontal shear flow with a free surface. *J. Fluid Mech.* **406**, 337–346.

Hughes, T. H. & Reid, W. H. 1965 On the stability of the asymptotic suction boundary-layer profile. *J. Fluid Mech.* **23**, 715–735.

Lamb, H. 1932 *Hydrodynamics*. Cambridge University Press.

Melville, W. K., Shear, R. & Veron, F. 1998 Laboratory measurements of the generation and evolution of Langmuir circulations. *J. Fluid Mech.* **364**, 31–58.

Miles, J. W. 1957 On the generation of surface waves by shear flows. *J. Fluid Mech.* **3**, 185–204.

Morland, L. C., Saffman, P. G. & Yuen, H. 1991 Waves generated by shear layer instabilities. *Proc. R. Soc. Lond.* A **413**, 441–450 (referred to herein as MSY).

Shrira, V. I. 1993 Surface waves on shear currents: solution of the boundary-value problem. *J. Fluid Mech.* **252**, 565–584.

Yih, C. S. 1972 Surface waves in flowing water. *J. Fluid Mech.* **51**, 209–220.